

# Magneto-optical constants of fluoride optical crystals and other AB<sub>2</sub> and A<sub>2</sub>B type compounds

Egberto Munin,\* Carmen B. Pedroso and Antonio Balbin Villaverde

Instituto de Física Gleb Wataghin, Universidade Estadual de Campinas, Unicamp 13083-970, Campinas, São Paulo, Brasil

Measurements of the magneto-optical rotation at visible wavelengths for the optical crystals MgF<sub>2</sub>, CaF<sub>2</sub>, SrF<sub>2</sub>, BaF<sub>2</sub> and PbF<sub>2</sub> are reported. A pulsed magnetic field between 50 and 80 kG was used. The PbF<sub>2</sub> crystal was shown to be a good choice for the construction of optical isolators operating in the near UV. From the data, the magneto-optic anomaly factor  $\gamma$  for each sample was calculated and magneto-optic constants reported in the literature for other compounds with the general formulae AB<sub>2</sub> and A<sub>2</sub>B were compiled. The magneto-optic anomaly factors for these types of materials are analysed in terms of Pauling's electronegativity.

The Faraday effect in transparent solid-state materials has been extensively investigated over the last decade,<sup>1–6</sup> motivated by the continued development and present use of the optical technology. The Faraday effect, a phenomenon which manifests as a magnetically induced rotation of the plane of the polarization of light propagating through a medium, has widespread practical application in the construction of miniature, fibre-integrated optical isolators for use in optical communication systems<sup>7</sup> and large-aperture optical isolators used to cut feedback in oscillator-amplifier chains in table-top laser systems.<sup>8–11</sup> When an optical isolator is placed inside a laser cavity with a ring geometry, a unidirectional photon flux will be forced in such a resonator.<sup>12,13</sup> The Faraday effect has also been used in the construction of magnetic-field sensors,<sup>14,15</sup> non-contact transducers for the measurement of electric current in high-voltage transmission lines<sup>16–18</sup> and narrow line filters for laser frequency stabilization.<sup>2,19</sup> More recently, a tunable bandpass filter for use in near-infrared tunable lasers has been proposed.<sup>20</sup> Within the scope of basic materials research, the study of magneto-optical rotatory dispersion in semiconductors and insulators has often been used to study the nature of the corresponding optical transitions and the magnitude of the energy gap between bands.<sup>3,5,21–23</sup>

In this work we present measurements of the magneto-optical rotatory dispersion of AF<sub>2</sub> type fluoride crystals (A = Mg, Ca, Ba, Sr and Pb). Theoretical expressions developed on a classical and quantum-mechanical basis by Boswarva *et al.*<sup>21</sup> and Kolodziejczak *et al.*<sup>22</sup> are applied to describe the observed spectral behaviour of the rotation and to calculate the energy gap for these crystals. From the measured Verdet constants we calculate the magneto-optic anomaly factor ( $\gamma$ ) for the above fluorides. The published magneto-optical constants for other binary compounds of the AB<sub>2</sub> and A<sub>2</sub>B types are revised and included for completeness. The values of the magneto-optic anomaly factor of the families of compounds considered are analysed on the basis of Pauling's electronegativity scale. The anomaly factor, which has values between zero and unity, has usually been qualitatively correlated to the nature of the electronic bonding in the molecules.<sup>24</sup> When we plot the values of the  $\gamma$  constant against the difference of electronegativity between atoms A and B in the compounds above, we obtain (to our knowledge) the first observed correlation between this constant and a basic chemical property of the atoms.

## Theoretical concepts

Michael Faraday discovered that the plane of polarization of the light rotates when transmitted through a sample of

material subjected to a magnetic field. Although Faraday used a piece of glass in his original experiment, magneto-optical rotation was subsequently observed in all types of molecules. The microscopic origin of such rotation of polarized light is the inequality in the refractive index  $n_-$  and  $n_+$  for the left and right circularly polarized components into which a linearly polarized light could be resolved. Such an inequality arises from the magnetically induced splitting of the ground- and/or excited-state energy levels. The Faraday effect is a non-reciprocal phenomenon in which the rotation angle  $\theta$  depends on the wavelength  $\lambda$  and on the optical path length  $l$  in the medium

$$\theta = \frac{\pi}{\lambda} (n_+ - n_-)l \quad (1)$$

When written as a function of the strength of the applied field  $H$ , the following relationship holds for the amount of rotation  $\theta$

$$\theta = V l H \cdot u \quad (2)$$

where  $u$  is a unit vector in the direction of light propagation and  $V$  is a constant of proportionality known as the Verdet constant, which is characteristic of the material. For most materials, this constant may be given by the so-called modified Becquerel formula, derived from classical principles

$$V = \frac{e}{2mc^2} \gamma \lambda \frac{dn}{d\lambda} \quad (3)$$

where  $e$  and  $m$  are the electronic charge and mass, respectively, and  $c$  is the velocity of light. The factor  $\gamma$ , first introduced into the Becquerel equation by Darwin and Watson,<sup>25</sup> is referred to as the magneto-optic anomaly factor. Ramaseshan<sup>24</sup> has considered the relationship between this anomaly factor and the nature of the electronic bonding in certain cubic crystals. He indicated that the  $\gamma$  factor would have a value close to unity for predominantly ionic bonding and a deviation of its value from unity would indicate a certain amount of covalent character. Since Ramaseshan's work, there has been little additional study towards a better understanding of this factor. In the present study, we make use of the principles established by Linus Pauling,<sup>26</sup> who gives the percentage ionic character of a bond as a function of the difference of electronegativity  $\Delta\chi = |\chi_A - \chi_B|$  of the atoms A and B participating in the bond. The greater the difference in electronegativity, the greater is the ionic character of the bond.

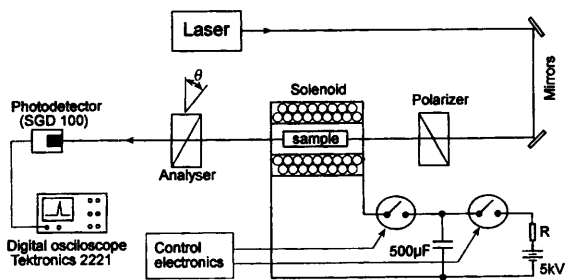


Fig. 1 Basic experimental setup for measurement of Faraday rotation using a pulsed magnetic field

## Experimental methods

The basic experimental setup for the measurement of the magneto-optical rotatory dispersion of the fluoride crystal samples is shown in Fig. 1. A pulsed magnetic field is produced by discharging a 500  $\mu\text{F}$  capacitor bank through an air-core solenoid. This solenoid consisted of 140 turns of copper wire wound in an eight-layer configuration with an inner diameter of 25 mm and a length of *ca.* 32 mm. The measured solenoid inductance was 384  $\mu\text{H}$ , which produced pulses with a duration of 1.5 ms at its base. The capacitor bank could be charged up to 5000 V. The field produced at the centre of the solenoid was approximately 26.5  $\text{G V}^{-1}$ . The measurements were performed at room temperature. To prevent heating the sample, the system was operated at a slow repetition rate and the solenoid was refrigerated by forced air. In addition, the sample was mounted such that it was mechanically isolated from the magnet, thus avoiding sample vibrations during the high-energy discharges. As light sources, we used an Innova-70 argon ion laser, manufactured by Coherent Inc. and a 1 mW, red helium–neon laser from Uniphase.

We used the null technique for the measurement of the magneto-optical rotation. The sample to be measured is placed in the centre of the solenoid. The linearly polarized laser beam passes sequentially through the sample and through an analyser. The temporal evolution of the optical signal after the analyser, during the magnetic-field pulse, is detected by a silicon photodiode and the corresponding electrical signal is captured by a digitizing oscilloscope. For a given sample, the analyser is shifted from the zero-field null position by a certain angle  $\theta$  conveniently chosen. The magnetic field required to recover the null position is then determined after a sequence of discharges with varying voltage at the capacitor bank. Knowing the magnetic-field intensity required to rotate the polarization by the preset angle  $\theta$ , the Verdet constant is calculated using eqn. (2). The magnetic field at the centre of the solenoid is calibrated at the peak of the pulse using a piece of FR-5 glass approximately the same length as that of the samples (*ca.* 1 cm). We adopted a value of 0.245  $\text{min G}^{-1} \text{cm}^{-1}$  for the Verdet constant of this glass,

which corresponds to the average of the data reported in the literature<sup>27,28</sup> for the He–Ne laser wavelength.

## Results

We measured the magneto-optical rotatory dispersion of five fluoride crystals of the type  $\text{AF}_2$ . These crystals, supplied by the Harshaw Chemical Company, Solon, OH, are calcium fluoride ( $\text{CaF}_2$ ), barium fluoride ( $\text{BaF}_2$ ), strontium fluoride ( $\text{SrF}_2$ ), magnesium fluoride ( $\text{MgF}_2$ ) and lead fluoride ( $\text{PbF}_2$ ). All have a cubic structure except for the magnesium fluoride which is a tetragonal crystal. The  $\text{MgF}_2$  crystal had the polished faces perpendicular to its optical axis. To minimize measurement errors which could be introduced by the birefringence of this crystal, the laser beam was aligned parallel to the optical axis using the Maltese-Cross method. This method consists of centring, with respect to the laser beam the interference pattern which is observed when such a uniaxial crystal is placed between crossed polarizers and illuminated by a point source emitting non-parallel light rays. In practice, such a point source may be simulated by scattering the laser light with a thin paper sheet placed close to the entrance face of the crystal. All the samples were rod shaped, 5 mm in diameter and 10 mm in length. The measurements were performed with field intensities ranging between 50 and 80 kG.

Table 1 gives the results of the Verdet constant measurements for the fluoride crystals at seven laser lines. The crystals are listed in increasing order of the Verdet constant. Also listed are the values of the magneto-optic anomaly factor  $\gamma$ , calculated at 632.8 nm using eqn. (3). The optical dispersion  $\text{dn}/\text{d}\lambda$  was obtained for each crystal using the refractive-index data tabulated by Miles *et al.*<sup>29</sup> It can be seen from the data that the Verdet constant for the lead fluoride crystal is at least five times higher than the corresponding values for any of the alkaline-earth fluorides. Because of its high Verdet constant and good transparency, this crystal may be a good choice for the construction of optical isolators in the near UV  $\geq 300$  nm, since competing materials such as paramagnetic terbium glasses begin to absorb strongly in this spectral range. Among the alkaline-earth fluorides,  $\text{BaF}_2$  has the highest Verdet constant. Restricting ourselves to those alkaline-earth fluorides with cubic crystalline structure, the magneto-optical rotation is observed to increase with increasing atomic weight of the cation, *i.e.* in the order:  $\text{CaF}_2 < \text{SrF}_2 < \text{BaF}_2$ .

Based on a model of a single oscillator having a narrow resonance centred at the frequency  $\omega_0$ , the spectral dependence of the Faraday rotation, expressed by the Verdet constant, is given by<sup>30</sup>

$$nV = \frac{kx^2}{(1-x^2)^2} \quad (4)$$

where  $n$  is the index of refraction,  $k$  is a constant and  $x = \omega/\omega_0$ , where  $\omega$  is the frequency of the light. A theory for the

Table 1 Verdet constant as a function of wavelength for fluoride crystals and  $\gamma$  factor calculated for each sample at He–Ne laser wavelengths

$\lambda/\text{nm}$	Verdet constant/ $\text{min G}^{-1} \text{cm}^{-1}$				
	$\text{CaF}_2$	$\text{MgF}_2$	$\text{SrF}_2$	$\text{BaF}_2$	$\text{PbF}_2$
632.8	0.00775	0.00810	0.00978	0.0131	0.0653
514.5	0.0120	0.0124	0.0151	0.0204	0.108
501.7	0.0127	0.0131	0.0158	0.0214	0.115
496.5	0.0130	0.0135	0.0162	0.0219	0.118
488.0	0.0136	0.0139	0.0168	0.0228	0.123
476.5	0.0142	0.0146	0.0178	0.0239	0.131
457.9	0.0154	0.0157	0.0193	0.0261	0.145
$\gamma$ factor at 632.8 nm	0.633	0.845	0.783	0.840	0.692

interband Faraday rotation was developed by Kolodziejczak, Lax and Nishina<sup>22</sup> using a semiclassical approach. They obtained for the case of phononless interband transitions the following relationship, hereafter referred to as the KLN model:

$$nV = \frac{k_1}{x} \left\{ [(1-x)^{-1/2} - (1+x)^{-1/2}] - \frac{4}{x} [2 - (1-x)^{1/2} - (1+x)^{1/2}] \right\} \quad (5)$$

where  $k_1$  is a constant independent of the frequency,  $x = E/E_g$ , where  $E = \hbar\omega$ , *i.e.* the incident photon energy, and  $E_g$  is the energy gap between the valence and conduction bands. There is another theoretical formula for the prediction of the interband Faraday rotation derived from a quantum-mechanical treatment by Boswarva, Howard and Lidiard (BHL).<sup>21</sup> The result of their calculation for direct interband transitions is expressed by

$$nV = k_2 \left\{ \frac{1}{x} [(1-x)^{-1/2} - (1+x)^{-1/2}] - 1 \right\} \quad (6)$$

The two formulae are very similar and both approach  $(1-x)^{-1/2}$  when the energy of the incident photons is close to the energy gap, *i.e.* when  $x \rightarrow 1$ . Both formulae were observed to fit to our experimental data. Their fit to the observed rotation spectra was carried out by allowing the two adjustable parameters  $E_g$  and  $k_1$  or  $k_2$  to vary. In Fig. 2 we plot the product  $nV$  against the wavelength for the alkaline-earth fluoride crystals and in Fig. 3 that for the  $\text{PbF}_2$  crystal. The fitting curves obtained using the BHL formula are represented by solid lines. Table 2 gives the values for the fitting parameters obtained with both the KLN and BHL models. The values of the energy gap obtained with the KLN theory are systematically higher than those obtained using the BHL expression. The observed differences between the  $E_g$  values given by the two models ranges from 11 to 15%, depending on the sample. Such a difference has also been observed in other studies reported previously.<sup>3,5</sup>

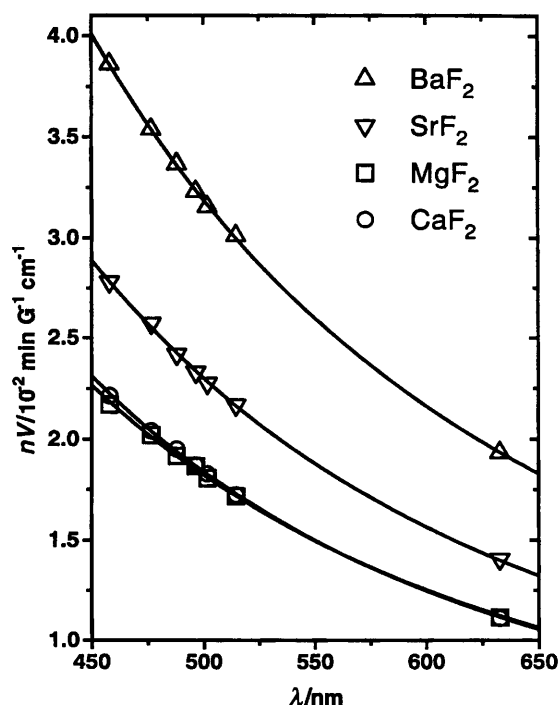


Fig. 2 Plot of the product  $nV$  versus wavelength for the alkaline-earth fluoride crystals; solid lines correspond to theoretical curves obtained using the BHL model [eqn. (6)]

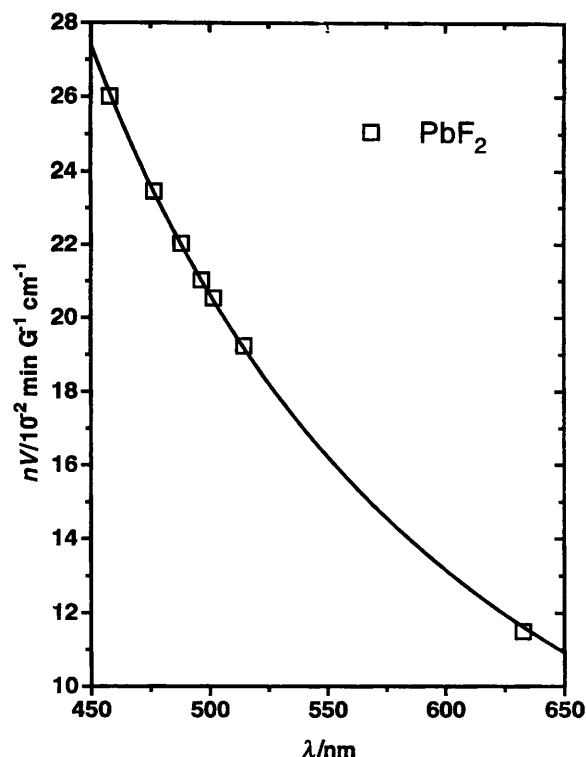


Fig. 3 Plot of the product  $nV$  versus wavelength for the lead fluoride crystal, solid line corresponds to the theoretical curve obtained using the BHL model [eqn. (6)]

The value of  $\gamma$  for the crystals we measured was observed to be nearly constant over the investigated spectral range, varying by less than 3% from 632.8 to 457.9 nm throughout, a variation which is close to the experimental uncertainties. The  $\gamma$  values for the fluoride crystals at the He-Ne laser wavelength are given in Table 1. For these crystals we found values ranging from 0.63 for  $\text{CaF}_2$  to 0.845 for  $\text{MgF}_2$ .

### Magneto-optical constants of materials with the general formulae $\text{AB}_2$ and $\text{A}_2\text{B}$

A better analysis of the magneto-optical constants of the materials studied is possible if we consider our results together with literature data. For example, Table 3 gives the value of the magneto-optic anomaly factor published by Darwin and

Table 2 Faraday rotation parameters for BHL and KLN theoretical models

crystal	BHL		KLN	
	$E_g/\text{eV}$	$k_2$	$E_g/\text{eV}$	$k_1$
$\text{CaF}_2$	8.3 <sub>3</sub>	0.30 <sub>9</sub>	9.5 <sub>1</sub>	0.80 <sub>3</sub>
$\text{MgF}_2$	12.2 <sub>0</sub>	0.67 <sub>9</sub>	14.0 <sub>0</sub>	1.7 <sub>9</sub>
$\text{SrF}_2$	8.6 <sub>7</sub>	0.42 <sub>1</sub>	9.9 <sub>1</sub>	1.1 <sub>0</sub>
$\text{BaF}_2$	8.2 <sub>9</sub>	0.53 <sub>0</sub>	9.4 <sub>7</sub>	1.3 <sub>8</sub>
$\text{PbF}_2$	4.7 <sub>1</sub>	0.92 <sub>4</sub>	5.2 <sub>3</sub>	2.2 <sub>6</sub>

Table 3 Values for the  $\gamma$  constant at 589 nm reported in ref. 25 for various compounds of the type  $\text{AB}_2$  and  $\text{A}_2\text{B}$

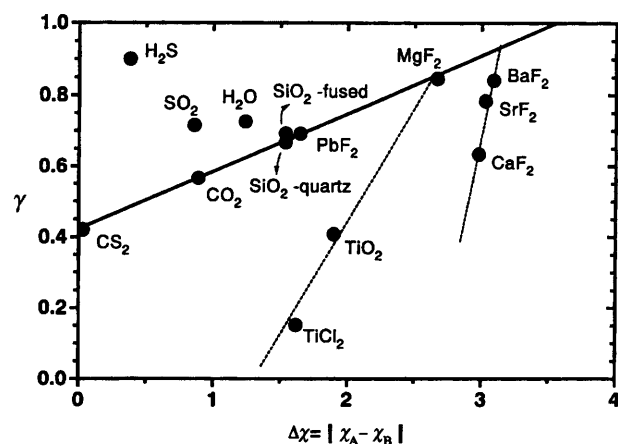
material	$\gamma$
$\text{SiO}_2(\text{quartz})$	0.667
$\text{H}_2\text{O}$	0.68
$\text{CO}_2$	0.566
$\text{CS}_2$	0.42

**Table 4** Values of the  $\gamma$  factor calculated from published values of the Verdet constant and optical dispersion for various compounds of the type  $AB_2$  and  $A_2B$ 

material	$V$ /min $G^{-1} cm^{-1}$	wavelength/nm	ref. for Verdet constant	ref. for optical dispersion	$\gamma$
TiO <sub>2</sub>	-0.1536	589	31	32	0.408
TiCl <sub>2</sub>	-0.0152	589	33	33	0.151
SiO <sub>2</sub> (fused)	0.01197	632.8	5	34	0.692
H <sub>2</sub> O	0.0115	632.8	35	36	0.771
SO <sub>2</sub>	0.5893	589	37	38	0.716
H <sub>2</sub> S	$41.5 \times 10^{-6}$	578	39	38	0.901

Watson<sup>25</sup> for some substances with the general formulae  $AB_2$  and  $A_2B$  and Table 4 gives the magneto-optic anomaly factor for other similar compounds, calculated by us based on published data for the Verdet constant and optical dispersion. The compiled values together with the experimental data obtained in this work for the fluoride crystals are plotted in Fig. 4 against the difference of electronegativity  $\Delta\chi = |\chi_A - \chi_B|$ , which is a measure of the ionic character of a bond. For water, we averaged the values given in Tables 3 and 4, as they differ from each other by more than 10%. It is interesting to note that the materials which lie on the solid line in Fig. 4 are those having molecular collinear bonds when in the vapour or liquid states. This solid line divides the plot into two regions. In the region above the solid line are non-solid, polar materials. Underneath the solid line, we observe only crystalline materials. The dividing line itself contains materials in liquid, gaseous, crystalline and amorphous phases. In the region occupied by crystalline materials, we can observe two well defined branches. One corresponds to those crystals of octahedral structure: MgF<sub>2</sub>, TiO<sub>2</sub> and TiCl<sub>2</sub>, while the other contains the three alkaline-earth fluorides of cubic structure measured in this work, which depart from the solid line as the molecular bond angle observed in the vapour state increases. These bond angles, given by Wells,<sup>40</sup> are 100° for BaF<sub>2</sub>, 108° for SrF<sub>2</sub> and 140° for CaF<sub>2</sub>.

Cole<sup>41</sup> showed that the Verdet constant for a number of optical glasses may be correlated to the commonly used Abbe number  $(n_D - 1)/(n_F - n_C)$  where  $n_D$ ,  $n_C$  and  $n_F$  denote the refractive index at 587.56, 656.28 and 486.13 nm, respectively. In a later work, Weber<sup>6</sup> plotted the Verdet constant for a number of silicate glasses against the partial dispersion  $(n_D - n_C)$ . He observed a good correlation when fitting the data to a straight line. In the present work we attempted to verify this relationship for the families of materials studied, but no such correlation was evident. We observed that a similar correlation could be obtained for compounds other than

**Fig. 4** Magneto-optic anomaly factor for various substances of the type  $AB_2$  and  $A_2B$ , plotted as a function of the difference of electronegativity between atoms A and B

glasses only when we select a group of materials having a narrow range of values for the magneto-optic anomaly factor. This may be easily understood in the light of eqn. (3). It should be expected that such a correlation would be valid only within some restricted families of materials, for example, a family of glasses with a predominantly silicate composition, as in ref. 6.

## Conclusion

In summary, we measured the Verdet constant as a function of the wavelength for five fluoride crystals: BaF<sub>2</sub>, SrF<sub>2</sub>, CaF<sub>2</sub>, MgF<sub>2</sub> and PbF<sub>2</sub>. The results show that the PbF<sub>2</sub> crystal is a good magneto-optical rotator and could be used in optical isolators operating in the near UV. The magneto-optic anomaly factor for these crystals was calculated using optical dispersion data found in the literature. Data for other substances having the general formulae  $AB_2$  and  $A_2B$  have been compiled and presented. We have shown that there is a correlation between the magneto-optic anomaly factor and the difference of electronegativity between the ions A and B which participate in the bond.

The authors gratefully acknowledge financial support from the Fundação de Amparo a Pesquisa do Estado de São Paulo (FAPESP), Conselho Nacional de Desenvolvimento Científico e Tecnológico (CNPq) and Financiadora de Estudos e Projetos (FINEP).

## References

- N. P. Barnes and L. B. Petway, *J. Opt. Soc. Am. B: Opt. Phys.*, 1992, **9**, 1912.
- H. Y. Ling, *J. Opt. Soc. Am. A*, 1994, **11**, 754.
- E. Munin and A. B. Villaverde: *J. Phys. Condens. Matter*, 1991, **3**, 5099.
- H. Guerrero, J. L. Escudero and E. Bernabeu, *Opt. Lett.*, 1992, **17**, 760.
- E. Munin, J. A. Roversi and A. B. Villaverde, *J. Phys. D: Appl. Phys.*, 1992, **25**, 1635.
- M. J. Weber, *Proc. SPIE-Int. Soc. Opt. Eng.*, 1986, **681**, 75.
- D. K. Wilson, *Laser Focus World*, 1991, **27**, 175.
- P. A. Schulz, *Appl. Opt.*, 1989, **28**, 4458.
- J. A. Wunderlich and L. G. DeShazer, *Appl. Opt.*, 1977, **16**, 1584.
- D. J. Gauthier, P. Narum and R. W. Boyd, *Opt. Lett.*, 1986, **11**, 623.
- A. B. Villaverde, *J. Phys. E: Sci. Instrum.*, 1981, **14**, 1073.
- T. F. Johnson Jr. and W. Proffitt, *IEEE J. Quantum Electron.*, 1980, **16**, 483.
- P. A. Schulz, *IEEE J. Quantum Electron.*, 1988, **12**, 1039.
- J. Malecki, M. Surma and J. Gibalewickz, *Acta Phys. Pol.*, 1957, **16**, 151.
- M. N. Deeter, A. H. Rose and G. W. Day, *J. Lightwave Technol.*, 1990, **8**, 1838.
- A. H. Rose, M. N. Deeter and G. W. Day, *Opt. Lett.*, 1993, **18**, 1471.
- Y. N. Ning and D. A. Jackson, *Opt. Lett.*, 1993, **18**, 835.
- N. C. Pistoni and M. Martinelli, *Opt. Lett.*, 1993, **18**, 314.
- P. Wanninger, E. C. Valdez and T. M. Shay, *IEEE Photon Technol. Lett.*, 1992, **4**, 94.
- E. Munin, *IEEE Trans. Magn.*, 1996, **32**, 316.



- 21 I. M. Boswarva, R. E. Howard and A. B. Lidiard, *Proc. R. Soc. London Ser. A*, 1962, **269**, 125.
- 22 J. Kolodziejczak, B. Lax and Y. Nishina, *Phys. Rev.*, 1962, **128**, 2655.
- 23 M. Balkanski, E. Amzallag and D. Langer, *J. Phys. Chem. Solids*, 1966, **27**, 299.
- 24 S. Ramaseshan, *Proc. Indian Acad. Sci. A*, 1948, **28**, 360.
- 25 C. G. Darwin and W. H. Watson, *Proc. R. Soc. London Ser. A*, 1927, **114**, 474.
- 26 L. Pauling, *The Nature of the Chemical Bond*, Cornell University Press, New York, 3rd edn., 1960.
- 27 Hoya Faraday Rotator Glass Report, Hoya Optics Inc., Tokio, 1974.
- 28 I. Ioshino, *Jpn. J. Appl. Phys.*, 1980, **19**, 7451.
- 29 P. A. Miles, M. J. Dodge, S. S. Ballard, J. S. Browder, A. Feldman and M. J. Weber, in *CRC Handbook of Laser Science and Technology*, ed. M. J. Weber, CRC Press Inc., Boca Raton, FL, 1986, vol IV, pp. 24–41.
- 30 W. Grevendonk, L. Van Den Abeele, P. Van den Keybus, B. Vanhuysse and G. Ruymbeek, *Phys. Stat. Solidi B*, 1981, **108**, K53.
- 31 W. S. Baer, *J. Phys. Chem. Solids*, 1967, **28**, 677.
- 32 D. C. Cronmeyer, *Phys. Rev.*, 1952, **87**, 876.
- 33 M. H. Becquerel, *Comptes Rendus*, 1897, **125**, 679.
- 34 *Dynasil Synthetic Fused Silica Catalogue 302M*, Dynasil Corporation, Berlin, NJ.
- 35 A. Balbin Villaverde and D. A. Donatti, *J. Chem. Phys.*, 1979, **71**, 4021.
- 36 W. E. Forsythe, *Smithsonian Physics Tables*, Washington, 9th edn., 1969, pp. 530.
- 37 L. R. Ingersoll and D. H. Liebenberg, *J. Opt. Soc. Am.*, 1958, **48**, 339.
- 38 J. J. Fox and F. G. H. Tate, in *International Critical Tables of Numerical data, Physics, Chemistry and Technology*, ed. E. W. Washburn, McGraw Hill, New York, 1st edn., 1930, vol. VII, pp. 01.
- 39 W. R. Cook, Jr. and H. Jaffe, in *American Institute of Physics Handbook*, ed., D. E. Gray, McGraw Hill, New York, 3rd edn., 1972, ch. 6, p. 230.
- 40 A. F. Wells, *Structural Inorganic Chemistry*, Oxford University Press, Oxford, 5th edn., 1984.
- 41 H. Cole, *J. Soc. Glass Technol.* 1950, **34**, 220.

Paper 5/08378H; Received 28th December, 1995